

Received November 29, 2019, accepted December 6, 2019, date of publication December 12, 2019, date of current version December 23, 2019.

Digital Object Identifier 10.1109/ACCESS.2019.2959130

# Compact Base Station Antenna Based on Image Theory for UWB/5G RTLS Embraced Smart Parking of Driverless Cars

ABUBAKAR SHARIF<sup>1,4</sup>, JINHAO GUO<sup>1</sup>, JUN OUYANG<sup>1</sup>, SHENG SUN<sup>1</sup>, (Senior Member, IEEE), KAMRAN ARSHAD<sup>2</sup>, (Senior Member, IEEE), MUHAMMAD ALI IMRAN<sup>3</sup>, (Senior Member, IEEE), AND QAMMER H. ABBASI<sup>3</sup>, (Senior Member, IEEE)

<sup>1</sup>School of Electronic Science and Engineering, University of Electronic Science and Technology of China, Chengdu 611731, China

<sup>2</sup>Faculty of Engineering, Ajman University, Ajman, United Arab Emirates

<sup>3</sup>School of Engineering, University of Glasgow, Glasgow G12 8QQ, U.K.

<sup>4</sup>Electrical Engineering Department, Government College University Faisalabad (GCUF), Faisalabad 38000, Pakistan

Corresponding author: Jun Ouyang (yjou@uestc.edu.cn)

This work was supported in part by the UESTC Research Funding under Grant Y03019023601016278 and in part by the Ajman University Internal Research Grant.

**ABSTRACT** The Internet of Thing (IoT) and fifth-generation mobile communication networks (5G) are leading towards a paradigm shift by providing seamless connectivity to a large number of devices. The applications of IoT in smart cities have further attracted local authorities to adopt technologies such as driverless cars, smart parking and smart waste management. This paper presents a compact base station antenna design with enhanced directivity/gain for ultra-wideband (UWB)/5G embraced real-time location systems (RTLS) based smart parking of driverless cars. The proposed base station antenna is based on image theory to achieve enhanced directivity and narrower beam width without using more array elements to keep smaller dimensions. Moreover, the base station antenna consists of an antipodal dipole printed on the opposite side of Rogers 4350 substrate, and a metal plate carefully designed and placed to produce a mirror image in order to achieve a high value of directivity in a specified direction. The advantage behind the antipodal dipole configuration is to avoid the use of extra balun for impedance matching. The half-power beamwidth of  $110^\circ$  is achieved along with 7 dB gain by placing a reflector plane at the distance of  $0.25 \lambda_0$  from the proposed antipodal dipole antenna. Also, this antenna provides a bandwidth ranging from 6 to 7.25 GHz, which can be used for UWB or 5G based RTLS systems. Furthermore, the proposed compact antenna design will help to improve the localization accuracy of ultra-wideband RTLS systems for smart parking applications of autonomous cars.

**INDEX TERMS** Antenna design, bandwidth, directivity enhancement, driverless cars, Internet of Thing (IoT), Smart Cities.

## I. INTRODUCTION

5G mobile communication technology in collaboration with Internet of Things (IoT) producing a paradigm shift by providing connectivity to billions of devices with enhanced data rate up to 100s of Mb/s and latency up to 1 ms [1], [2]. 5G is no longer a dream but becomes today's reality and realizes many abstract visualizations into veracity by innovating a huge number of applications such as remote healthcare

The associate editor coordinating the review of this manuscript and approving it for publication was Akram Alomainy<sup>1</sup>.

monitoring [3], remote surgery, autonomous or driverless cars, smart cities [4], [5], smart waste management, smart parking solutions, smart homes, smart spaces [6] and IoT. Also, the first 5G standardization milestone also known as 5G new radio (5G NR) has marked 5G as key backbone technology to enable to Internet of Everything (IoE). Therefore, 5G is not just an upgrade to previous cellular communication standards, but a revolution that will create evolutions by eliminating limitations towards access, bandwidth/speed, performance, and latency on worldwide connectivity [7], [8].

Moreover, the IoT technology is providing a platform that foresees a communication model by enabling daily life things/objects to communicate with each other and with the users [8], [9]. Also, these things will be equipped with small microcontrollers, transceivers, and protocols stacks to assist them to communicate and maintain their unique identity over the Internet. The IoT technology has further immersed the Internet even more pervasive by enabling easy access and connectivity to a wide variety of devices ranging from home appliances, surveillance cameras, sensors, actuators, vehicles, displays, and so on [10], [11].

Vehicles parking is one of the most critical issues in large urban areas and cities. A typical car is parked for an average of 23 hours a day and occupies several parking spaces ranging from a parking lot or on-street parking/roadside parking. Vehicles parking conflicts especially conflicts for on-street/roadside parking are major issues for city planners, designers, and officials. Such issues in on-street parking occurred either due to mismanagement in slot allocation or parking mismanagement. Moreover, with the invention of autonomous and driverless cars, this challenge will be magnified further. However, thanks to technologies such as IoT, 5G, RFID, GPS and UWB RTLS that enables concept of smart cities and smart vehicle parking management [12]–[19].

UWB based RTLS systems can able to provide decimeter level accuracy regarding positing and localization. Unlike other positioning technologies such as GPS Bluetooth or Wi-Fi, UWB technology uses RF signal's time difference of arrival (TDOA) or Time of Flight to estimates the distance between target and reference base station, that provides more accuracy with much more precise range measurement [12]. Moreover, the UWB signals are resistant to multipath effects and can be distinguished even in noisy environments. Also, since UWB technology utilizes low power that's why it does not produce interference with other radio communication systems [20]–[25]. In addition to this, 5G technology can also provide similar advantages regarding position accuracy and localization due to ultra-dense small cells [7], [26]. Fig. 1 shows the Difference between positioning accuracy of ultra-wideband or 5G based RTLS systems and other positioning technologies.

Antennas have a great influence on positing systems like any other communication technology. A directional antenna poses more advantages to UWB or 5G based RTLS systems, alongside a small footprint of antenna helps to reduce the cost and meet the space constraints. A UWB PIFA type antenna has been proposed for RTLS systems. Although the size of antenna is small, how it has omnidirectional radiation pattern with very low gain profile 2.678 dB [27]. Another antenna was proposed in [28] for RTLS applications. This antenna has very large footprint along with low radiation performance. Therefore, in this paper, a compact base station antenna design with enhanced directivity is proposed for ultra-wideband(UWB)/5G embraced real-time location systems (RTLS) based smart parking of driverless or

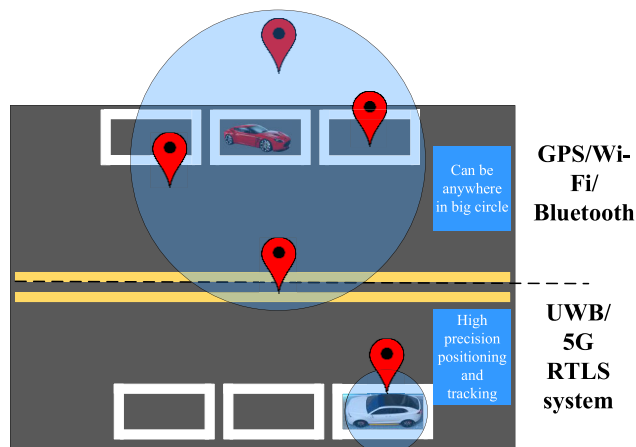
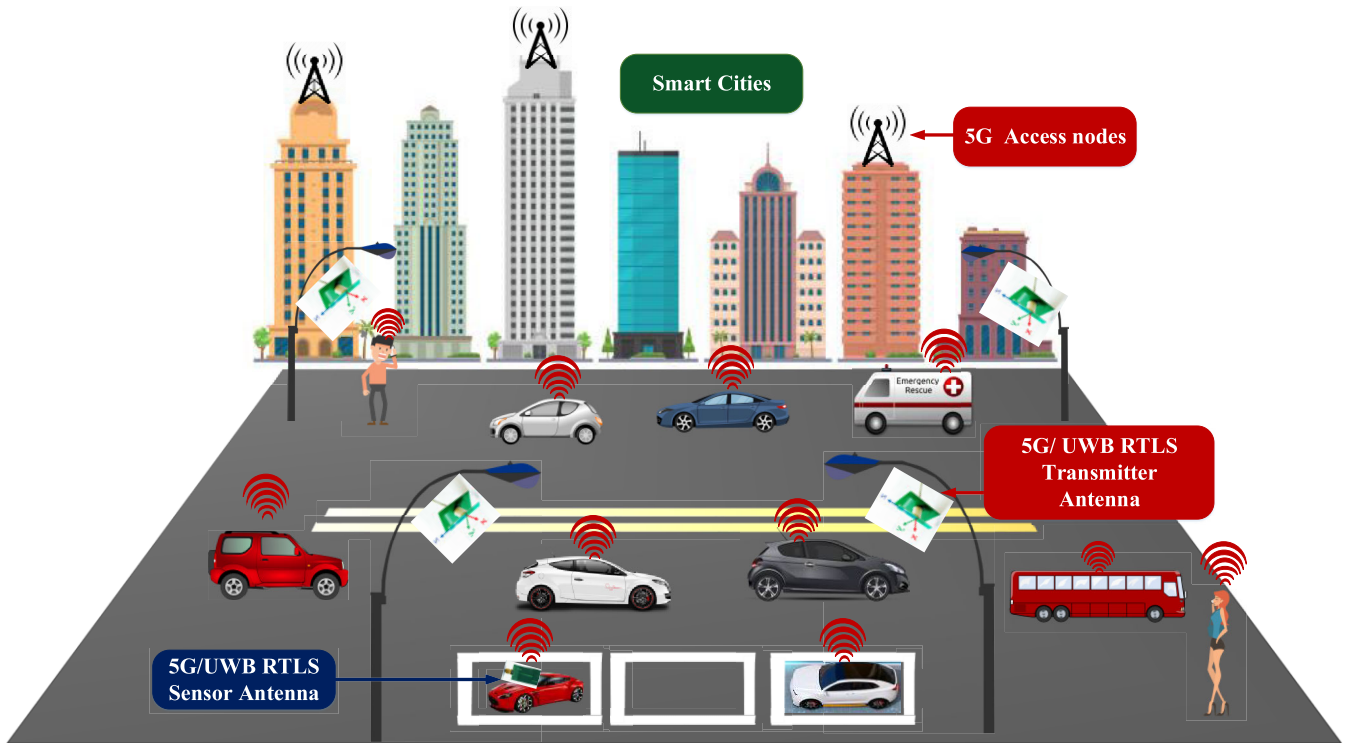


**FIGURE 1.** Difference between positioning accuracy of ultra-wideband or 5G based RTLS systems and other positioning technologies.

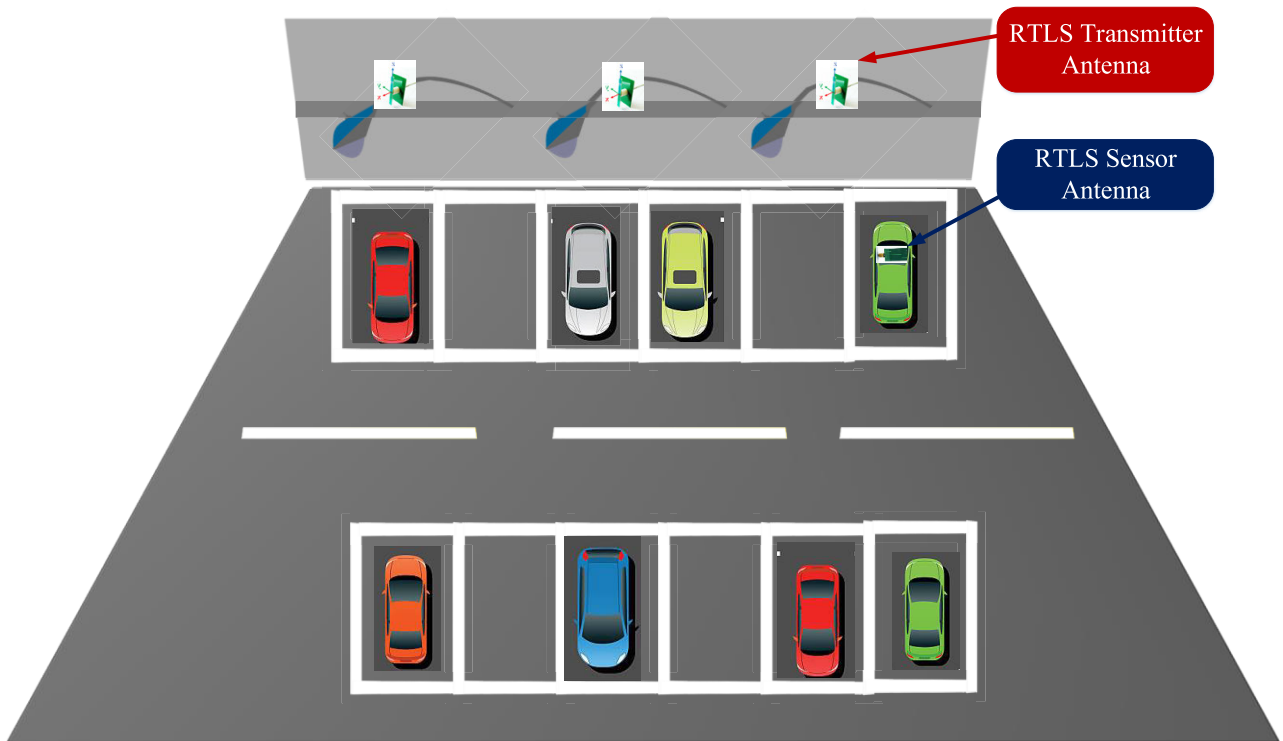
self-driving cars. The proposed base station antenna was based on image theory to achieve enhanced directivity and narrower beamwidth without using more number of array elements in order to keep smaller dimensions. Also, the base station antenna consists of antipodal dipole printed on the opposite side of Rogers 4350 substrate in order to avoid extra balun for impedance matching and a metal plate. The proposed design exploits image theory to produce mirror image in order to achieve high value of directivity in specified direction. This antenna provides 7 dB gain along with half-power beamwidth of  $110^\circ$  by placing a reflector plane at the distance of  $0.25\lambda_0$  from proposed antipodal dipole antenna. Also, this antenna offers a bandwidth ranging from 6 GHz to 7.25 GHz, which can be used for UWB or 5G based RTLS systems. Furthermore, the proposed compact antenna design will help to improve the localization accuracy of ultra-wideband RTLS systems for smart parking applications of autonomous cars or driverless cars.

## II. APPLICATION SCENARIO

Fig. 2 (a) illustrates the application scenario of the proposed base station antenna for on-street or roadside parking in smart cities applications. The proposed base station antenna design is mounted on preinstalled street light poles and the UWB sensor antennas will be either installed on autonomous car's rooftop or front windscreen. The sensor antenna will receive at least two base stations signals to determine its location and empty location on parking lot. Since the proposed antenna has enhanced directivity, so it provides high precision regarding position and localization for UWB or 5G based RTLS systems. Similarly, this antenna is suitable for smart underground parking systems (as shown in Fig. 2(b)) based on UWB or 5G RTLS, due to weak GPS signals availability in underground environments. Therefore, the proposed antenna based RTLS smart parking system will help a car to find an empty parking slot for itself along roadside or underground parking, guide it towards parking slot, and further help it to pay parking fees.



(a)



(b)

**FIGURE 2.** Application scenario of RTLS based base station and sensor antenna design in smart cities applications (a) For road-side or on-street parking of driverless cars (b) For underground parking of driverless or autonomous cars (Due to weak GPS signal underground RTLS based system provide more accurate positing and localization).

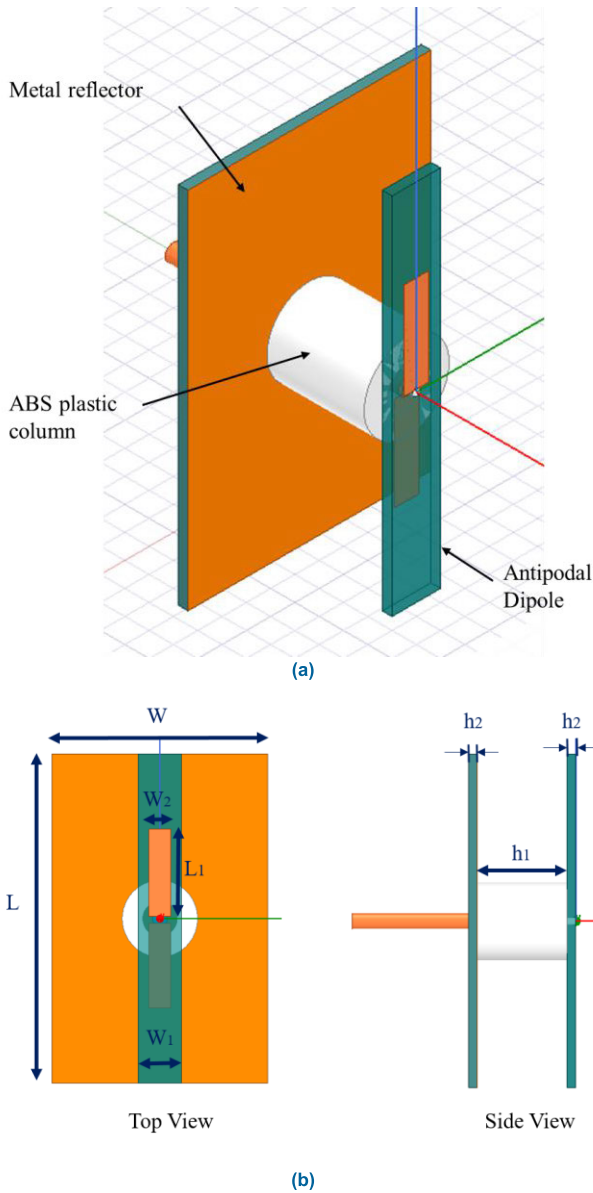


**FIGURE 3.** (a) Whole configuration proposed base station antenna design with ABS plastic column (b) Dimension of proposed base station antenna ( $L = 30$  mm,  $W = 20$  mm,  $L_1 = 7.95$  mm,  $W_1 = 4$  mm,  $W_2 = 2$  mm,  $h_1 = 8$  mm,  $h_2 = 0.8$  mm).

Furthermore, this antenna can be used in future 5G networks for localization of other objects such as human beings due to densely deployed access nodes.

### III. ANTENNA DESIGN METHODOLOGY AND REALIZATION

#### A. ANTENNA CONFIGURATION

The whole configuration and dimensions of the proposed base station antenna design are depicted in Fig. 3. It consists of an antipodal dipole fabricated on opposite sides of Roger 4350 substrate (as shown in Fig. 4), and a reflector metal plate etched Rogers 4350 substrate ( $\epsilon_r = 3.5$ ,  $\tan \delta = 0.0015$ ). The antipodal dipole part (which is quite similar to vintage

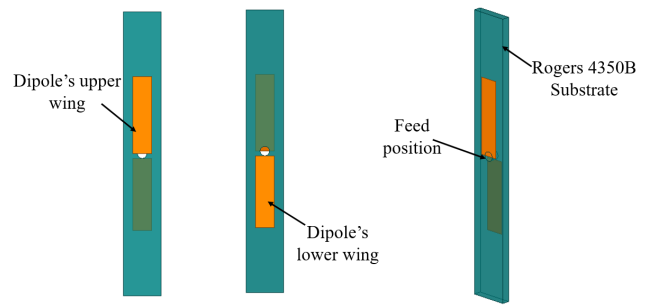


**FIGURE 4.** Antipodal dipole-like small patches fabricated on opposite sides of Roger 4350 substrate.

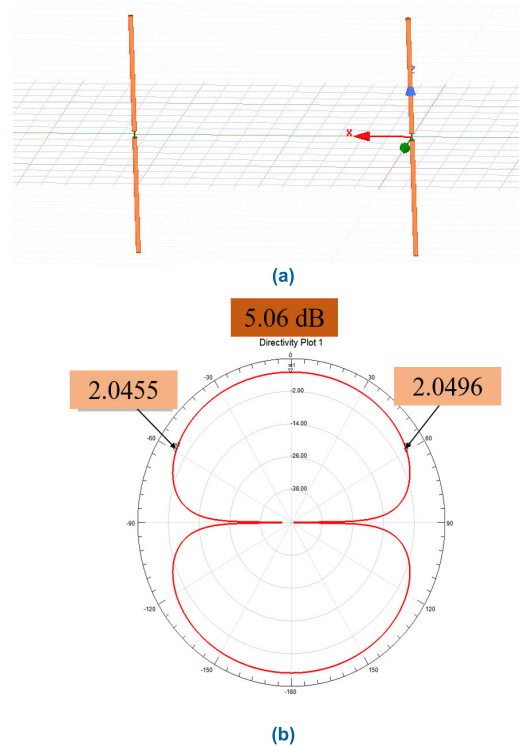


**FIGURE 5.** (a) Simulation model of two-element dipole array (b) Simulated radiation pattern of two-element dipole array.

airplane propeller fan) is differentially fed from one edge using single coaxial feedline. A small ABS plastic column was used to support the antenna structure, which was also included in antenna simulations and measurements.

#### B. DESIGN STEPS AND WORKING

The proposed antenna has been designed and optimized using HFSS at a center frequency of 6.5 GHz. The main aim of the proposed design was to achieve high directivity in order to get more localization accuracy for real-time locations systems. Along with this high directivity, the size of proposed design must be compact in order to meet the cost and space requirements. To increase the directivity of antenna, antenna array concept was used to attain high directivity in specific direction. Moreover, since the dipole is an array of current

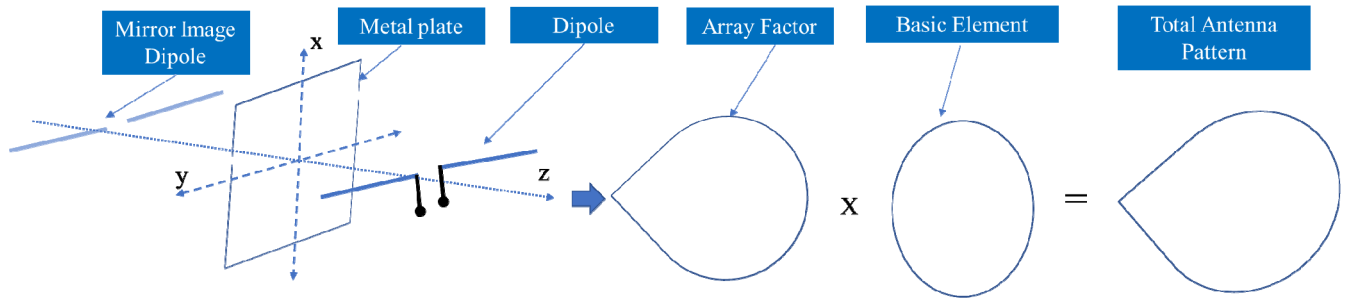


FIGURE 6. Dipole antenna placed in front of metal plate, it creates a mirror image dipole.

sources in the vertical direction, so we can consider using dipoles as the basic unit to achieve this goal. Therefore, starting with two-element dipole array with a half-wavelength spacing as shown in Fig. 5 (a). The half-power beamwidth and maximum gain associated with this two-element dipole array were 120° and 5 dB, respectively as illustrated in Fig. 5(b).

Due to space constraints, we use the metal plate instead of another dipole to increase directivity. An infinite metal was placed at  $0.25\lambda_o$  distance from the dipole. Due to the mirror image, it can be equivalent to an array of two dipoles as shown in Fig. 6.

The total Fairfield radiated by dipole and image dipole can be expressed as follows [29], [30]:

$$E_t = E_{dipole} + E_{image\_dipole} \quad (1)$$

$$E_t = E_o(\theta, \phi)e^{-j\varphi_o(\theta, \phi)} \sum_{i=1}^2 A_i e^{-j\varphi_o(\theta, \phi)} \quad (2)$$

The gain of the antenna array ( $G(\theta, \phi)$ ) can be expressed by taking square of (2) as follow:

$$G(\theta, \phi) \propto |E^2| = |E_o(\theta, \phi)|^2 \cdot \left| \sum_{i=1}^2 A_i e^{-j\varphi_o(\theta, \phi)} \right|^2 \quad (3)$$

where  $|E_o(\theta, \phi)|^2$  represents element factor that characteristics identical radiation pattern of dipole antenna elements, and

$\left| \sum_{i=1}^2 A_i e^{-j\varphi_o(\theta, \phi)} \right|^2$  represents an array factor.

As referred to [31], [32], the normalized far-field radiation pattern of the single half-wavelength dipole can be expressed as:

$$E(\theta, \phi) = \left[ \frac{\cos(\pi/2) \cos(\theta)}{\sin(\theta)} \right]^2 \quad (4)$$

The metal plate produces a virtual source due to the effect called image theory [32]. For analysis purposes only, these image sources generate exactly the same radiation pattern as original antenna above the ground plane, but 180° shifted.

Considering both the original dipole and image dipole, the normalized radiation pattern for this two-element array can be expressed as:

$$E_{2n}(\theta, \phi) = E_{2n}(\phi) = \sin^2((\pi/2) \sin(\phi)) \quad (5)$$

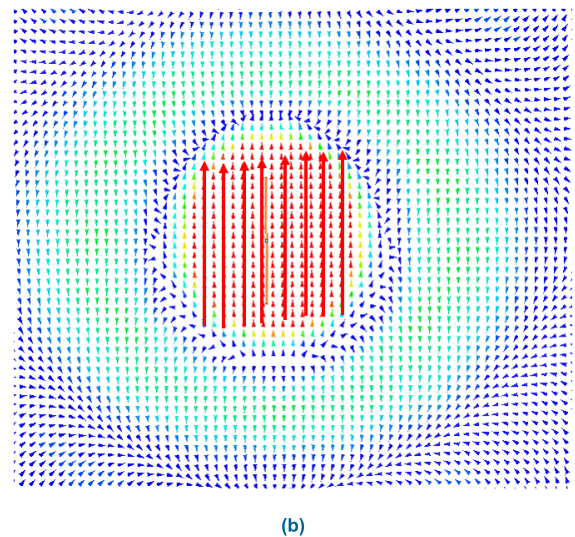
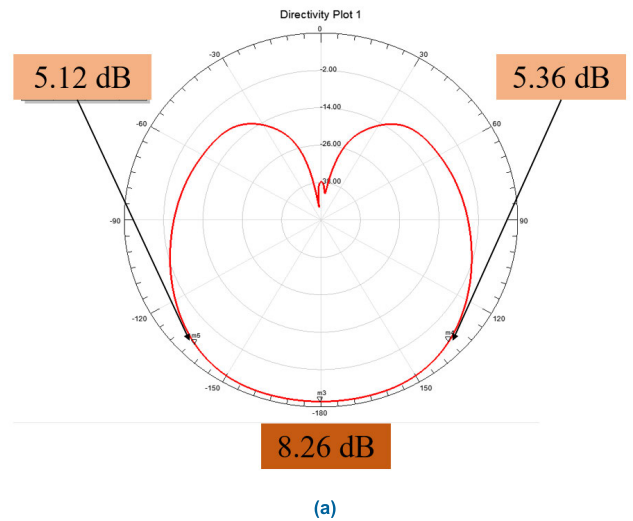


FIGURE 7. (a) Simulated radiation pattern resulted after placing infinite metal plate (b) Surface current distribution on infinite metal plate.

The simulated radiation pattern resulted after placing in the infinite metal plate is illustrated in Fig. 7 (a). The simulation results show that the maximum gain is 8.4 dB and the half-power beamwidth is about 90°.

Moreover, it can be observed that the maximum gain and beamwidth of the antipodal dipole with mirror metal plate are

different from those of two individual dipole array pattern. The reason behind this difference is because the electromagnetic waves generated by the dipoles excite current on the metal surface as shown in Fig. 7 (b). These currents on the metal surface can be regarded as an array of current sources in the vertical direction.

Consequently, this array of current sources increases the gain, while on the other hand produces a narrower beamwidth in the horizontal direction. Therefore, we can control the shape of the pattern by controlling the area of the metallic plane, and by changing the distribution of the current sources excited by the dipole on the metal floor.

Furthermore, a finite metal plate of dimensions 20 mm × 30 mm was placed behind the antipodal dipole instead of abstract conceptual infinite metal plate. The surface current distribution and radiation pattern resulted after placing the finite ground plane are depicted in Figs. 8(a) and (b), respectively. The current distribution again shows an array of current sources similar to the current sources generated in case of infinite ground plane. The maximum gain and beamwidth achieved in this case is 7.3 dB and 110°, which is little less as compared to maximum gain in case of infinite ground plane. However, the beamwidth and directivity resulted in case of finite ground plane are good enough and much better as compared to individual two-element dipole array.

Additionally, the simple dipole structure is replaced with an antipodal dipole, which has quite similar performance as simple dipole. The advantage behind this antipodal dipole configuration is to avoid the use of balun to feed the dipole antenna. In antipodal configuration, it is quite easier to feed the dipole using a simple coaxial feed line by connecting inner conductor to the one wing of antipodal dipole and outer conductor to another wing.

As shown in Fig. 9, the energy of the omnidirectional antenna (dipole antenna) is radiated in a 360° space. If we want to concentrate the energy of the omnidirectional antenna to the range of like 110°, its energy (directivity) must be described as follows:

$$D_1 = 2.15dB + 10 \log\left(\frac{360}{110}\right) = 7.3dB \quad (6)$$

So, the novelty of this work lies in getting the 110° beamwidth and 7dB gain with compact antenna size (20×30×8 mm<sup>3</sup>). The proposed design obtained so far have good gain and narrow beamwidth. However, the impedance bandwidth of antenna was just 0.55 GHz (8.5 %) as shown in Fig. 10 (a). For that reason, the measures are taken to increase the impedance bandwidth of the antenna to make it compatible with Decawave's DWM 1000 and DWM 1001 UWB transceivers [33], [34]. Because of the large induced current on the metallic plane, it affects the input impedance of the antenna. Also, the capacitance between the dipole and the metal plate was nullified by adding a small length of and the coaxial line. The coaxial line's inner and outer conductors are connected to the two wings of the dipole respectively, and the outer conductor of the coaxial line is also

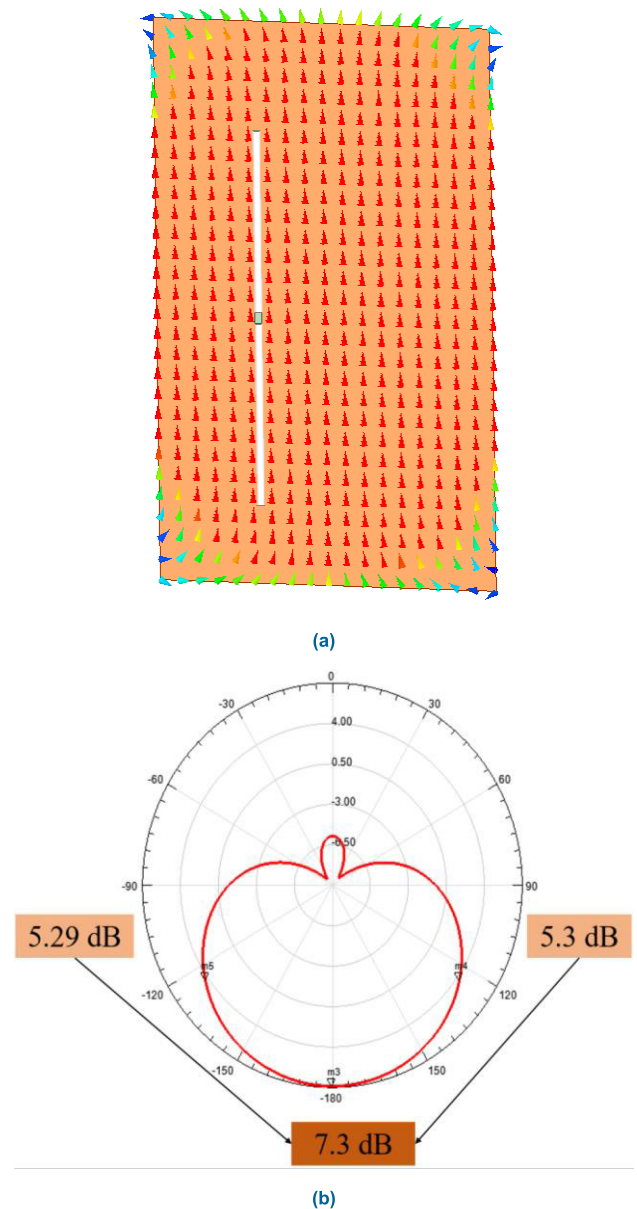


**FIGURE 8.** (a) Surface current distribution on a finite metal plate of surface area 30 × 20 mm (b) Simulated radiation pattern resulted after placing a finite metal plate.

connected to the metal plate. On one hand, this configuration creates ease of integration in feeding the dipole, on the other hand introduces an inductance, which is useful to compensate extra capacitance caused by the proximity of metallic plate.

In addition to this, the reactance between 6-7 GHz is greater than 0 at this time as depicted in Fig. 10 (b). Consequently, it is necessary to introduce a capacitance to reduce the reactance and thereby increase the bandwidth. As a result, the dipole is changed to a planar dipole to increase its facing area with the metal plate, thereby increasing the capacitance. Hence the antenna bandwidth is increased.

Moreover, a parametric study has been carried out to get optimal bandwidth by changing the width of the antipodal

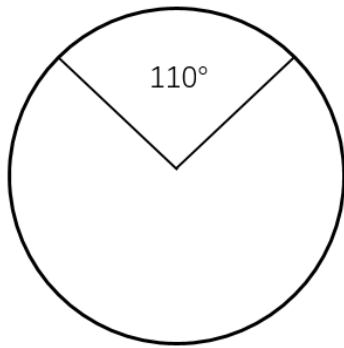
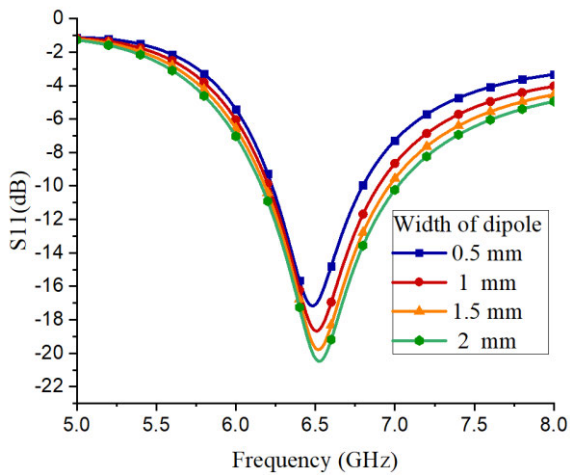
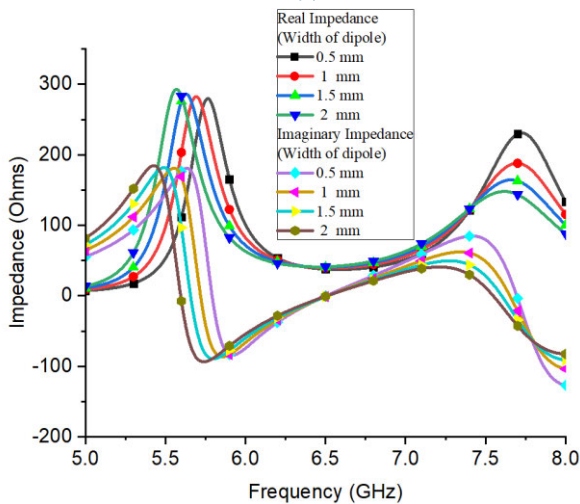


FIGURE 9. Representation of concentration of energy (directivity) from a simple dipole vs proposed antenna.



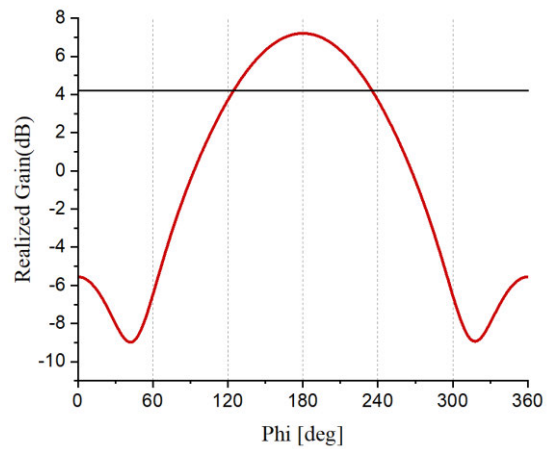
(a)



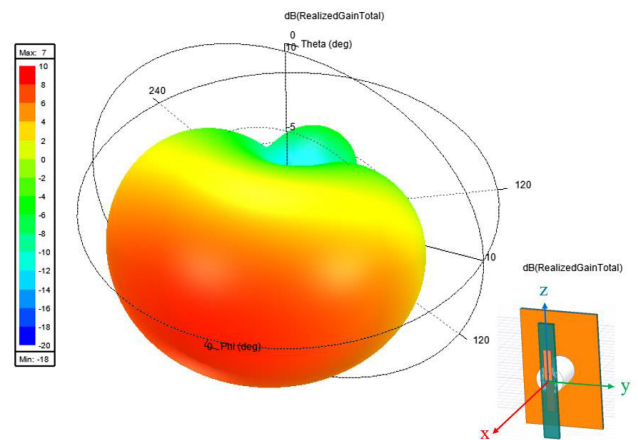
(b)

FIGURE 10. (a) Parametric study regarding S11 parameter of the proposed antenna as a function of width of antipodal dipole (b) Parametric study regarding Impedance of proposed antenna as a function of width of antipodal dipole.

dipole. Fig. 9 shows the plot of S11 parameter and impedance of whole antenna configuration with respect to dipole width. The bandwidth of proposed design increased gradually by



(a)



(b)

FIGURE 11. (a) Realized gain of proposed antenna design at 6.5 GHz (b) Simulated 3 D radiation pattern (realized gain) of proposed antenna design at 6.5 GHz.

increasing the width of antipodal dipole. The optimal bandwidth is achieved with dipole width of 2 mm.

Similarly, a flat impedance curve for the proposed antenna was achieved between 6 GHz to 7 GHz by setting the width of antipodal dipole 2mm. Therefore, the proposed antenna design poses 1 GHz bandwidth ranging from 6 GHz to 7.25 GHz (which is 15.5 %). Furthermore, Fig. 11 (a) shows the realized gain of proposed antenna design, which further clarifies the antenna performance in terms of radiation efficiency. The realized gain of antenna is also nearly 7 dB. Also, it is clarifying from Fig. 10 that half-power beamwidth point corresponds to Phi 123° and 233°, respectively endorsing the beamwidth of 110°. Moreover, the 3-D radiation pattern of proposed design at 6.5 GHz is shown in Fig. 11 (b).

IV. MEASUREMENT RESULTS AND DISCUSSION

A prototype of the proposed antenna was fabricated to prove the concept. The proposed antenna was fabricated using two layers of Rogers 4350 substrate with thickness (h = 0.8 mm).

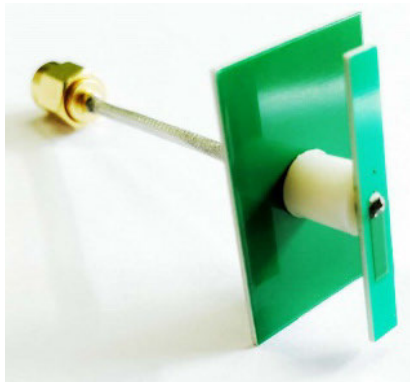


FIGURE 12. Photograph of the fabricated prototype of proposed antenna.

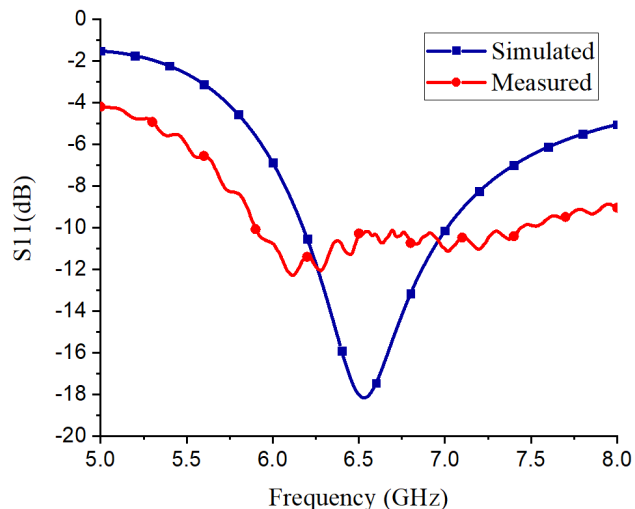


FIGURE 14. Measured and simulated S11 parameter of fabricated prototype of proposed antenna design.

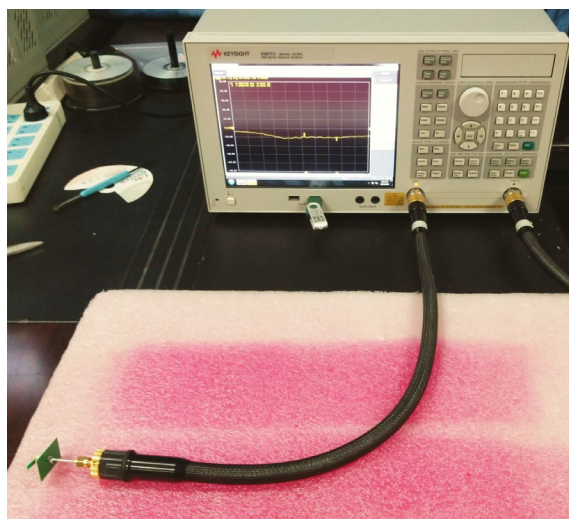


FIGURE 13. S11 parameter measurement of fabricated prototype using Vector Network Analyzer.

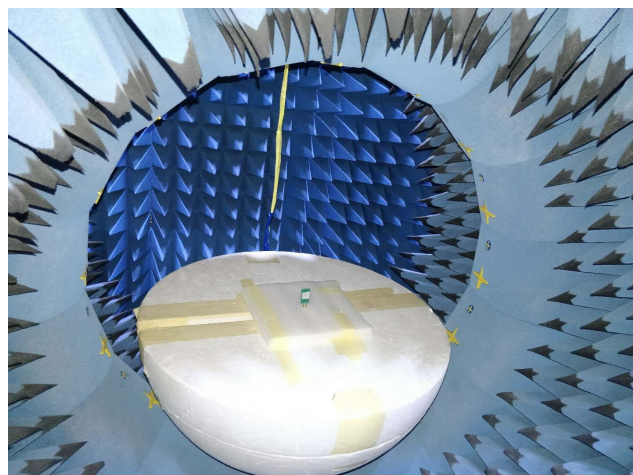


FIGURE 15. Radiation pattern and gain measurement of proposed antenna in an anechoic chamber.

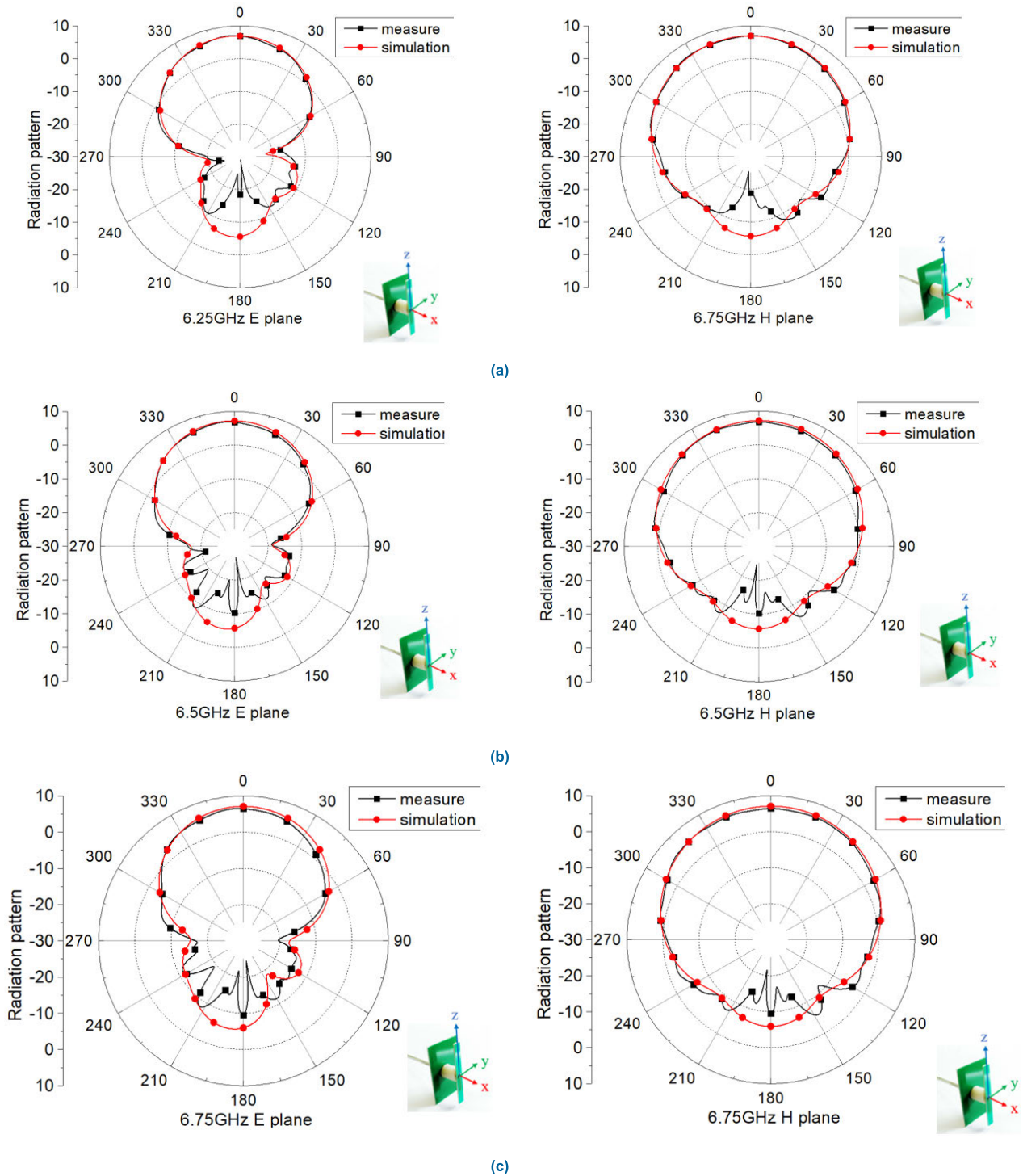
One layer of substrate was used to print antipodal dipole, with each wing of antipodal dipole on opposite sides of substrate. The metal plate is printed on second layer of substrate. A coaxial line is soldered with inner connector to one wing of antipodal dipole, while the outer connector with another wing of antipodal dipole. It is worth to mention here that antipodal dipole configuration avoids the use of extra balun for feeding as it is required in case of simple dipole.

Fig. 12 shows a fabricated prototype of proposed antenna design. Additionally, the fabricated antenna was attached with a vector network analyzer (Agilent E8363B) for S11 parameter measurements as shown in Fig. 13. The measured and simulated S11 parameter is shown in Fig. 14. As can be seen from Fig. 14, the measured S11 is less than -10 dB from 6.25 GHz to 7.25 GHz. Also, the measured result matched well with simulated one with little discrepancy, which may be resulted due to little bit shift in rated permittivity and loss tangent values of Rogers 4350 substrate.

It can be also noticed that there are some ripples in measured S11 parameter, especially in the higher band. This

phenomenon occurs partially due to the effects of the coaxial cables used in the measurement setup. Furthermore, the far-field radiation pattern of fabricated antenna prototype was also studied to verify the concept.

Fig. 15 shows the photograph of the fabricated antenna placed inside anechoic chamber for flexible antenna pattern and gain measurements. The anechoic chamber of dimensions (25 m × 15 m × 15 m) was established by SATIMO company. The simulated and measured H-plane and E-plane pattern of proposed antenna for 6.25 GHz, 6.5GHz, and 6.75 GHz are illustrated in Figs. 16 (a), (b) and (c), respectively. The measured radiation pattern results are matched well with simulated results. The antenna poses quite similar radiation characteristic performance for these three frequency bands, which proves the significance of proposed design in terms of stable radiation patterns for whole working frequency band. The E-plane and H-plane pattern revealed



**FIGURE 16.** (a) Simulated and measured E-plane and H-plane radiation pattern (realized gain) of proposed antenna design at 6.25 GHz (b) Simulated and measured E-plane and H-plane radiation pattern (realized gain) of proposed antenna design at 6.5 GHz (c) Simulated and measured E-plane and H-plane radiation pattern (realized gain) of proposed antenna design at 6.75 GHz.

that the proposed design has almost substantially equivalent beamwidth in both planes. More precisely, the beamwidth in H-plane is  $110^\circ$ , while the beamwidth in E-plane is even less than  $110^\circ$ , which means even more narrower beamwidth.

**V. IMPACT ON ACCURACY IMPROVEMENT**

To understand the impact of the proposed antenna design on localization improvement, we consider a scenario as depicted in Fig. 17, which shows proposed RTLS base station antenna

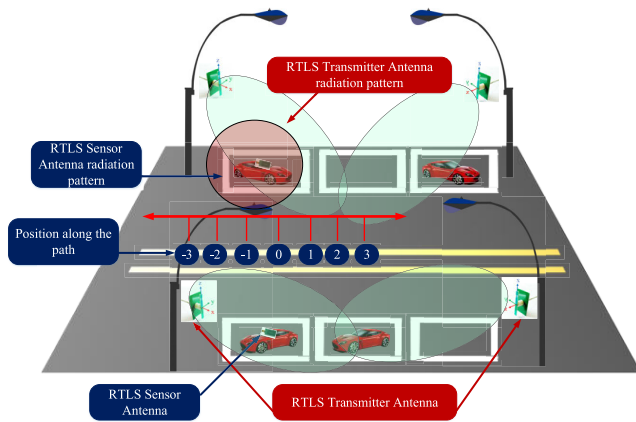


FIGURE 17. Scenario to view the impact of the antenna on localization accuracy improvement.

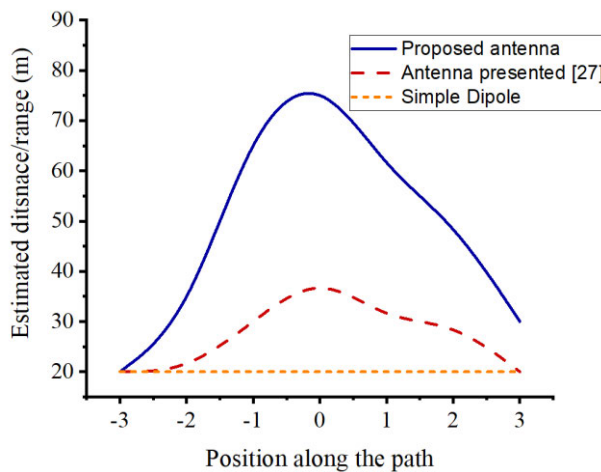


FIGURE 18. Comparison of estimated range of proposed antenna design plotted vs. different positions of sensor.

with enhanced directivity and a sensor tag antenna mounted on a car. Suppose the transmitter antenna radiates a signal with power  $P_t$ , and the signal received receiver antenna with power  $P_r$ .

The received power  $P_r$  can be computed using the Friis formula [29] in free space conditions as follows:

$$P_r = P_t \cdot G_t \cdot G_r \cdot PL \cdot \left( \frac{\lambda}{4\pi D} \right)^2 \quad (7)$$

where  $G_t$  and  $G_r$  are gains of the base station and sensor antennas, respectively,  $PL$  is polarization mismatch loss, and  $D$  is the distance between base station and sensor antennas.

The localization accuracy of the algorithm [35], [36] depends on estimation distance between transmitter and receiver antennas. This distance  $D$  can be calculated using received power as follows:

$$D = 10 \left( \frac{C - P_r}{10 \cdot n} \right) \quad (8)$$

where  $C$  corresponds to calibration factor and becomes equal to,  $P_r$  if base station and sensor antenna are aligned face to

face, and due to inverse of Friis formula  $n$  is equal to 2 [29]. If the directivity or gain of transmitter antenna increases up to 7 dB, which far much better than a simple dipole. So, the estimated distance (range) accuracy improvement [35] due to proposed antenna is illustrated in Fig. 18.

Fig. 18 summaries the estimated range, when the position of received sensor antenna is moved along the path. The estimated range due to proposed antenna is compared with antenna proposed in [27] and simple dipole antenna. As it can be observed, a considerable improvement in estimated distance due to the proposed antenna, which will further help localization algorithms to attain high accuracy in positioning and tracking. Therefore, the proposed antenna helps to improve the localization accuracy of 5G / UWB based RTLS systems.

## VI. CONCLUSION

In this paper presents, a compact base station antenna with enhanced gain/ directivity has been proposed for UWB/5G embraced RTLS based smart parking of driverless or self-driving cars. The image theory was exploited to get enhanced directivity and narrower beamwidth, instead of using more array elements in order to keep smaller dimensions. The base station antenna consists of antipodal dipole printed on opposite side of Rogers 4350 substrate, which avoids the use of extra balun for impedance matching. Moreover, a metal plate carefully designed and placed at a distance of  $0.25 \lambda_o$  from proposed antipodal dipole antenna to produce mirror image in order to achieve high value of directivity/gain. This antenna provides a bandwidth ranging from 6 GHz to 7.25 GHz proposed design along with 7 dB gain and  $110^\circ$  half-power beamwidth. Furthermore, the proposed compact antenna designs will help to improve the localization accuracy of UWB/5G based RTLS systems for smart parking applications of autonomous cars.

## REFERENCES

- [1] M. Shafi, A. F. Molisch, P. J. Smith, T. Haustein, P. Zhu, P. De Silva, F. Tufvesson, A. Benjebbour, and G. Wunder, "5G: A tutorial overview of standards, trials, challenges, deployment, and practice," *IEEE J. Sel. Areas Commun.*, vol. 35, no. 6, pp. 1201–1221, Jun. 2017.
- [2] D. Muirhead, M. A. Imran, and K. Arshad, "A survey of the challenges, opportunities and use of multiple antennas in current and future 5G small cell base stations," *IEEE Access*, vol. 4, pp. 2952–2964, 2016.
- [3] A. Rizwan, "A review on the role of nano-communication in future healthcare systems: A big data analytics perspective," *IEEE Access*, vol. 6, pp. 41903–41920, 2018.
- [4] M. A. Rodriguez-Hernandez, A. Gomez-Sacristan, and D. Gomez-Cuadrado, "SimulCity: Planning communications in smart cities," *IEEE Access*, vol. 7, pp. 46870–46884, 2019.
- [5] A. Zanello, N. Bui, A. Castellani, L. Vangelista, and M. Zorzi, "Internet of Things for smart cities," *IEEE Internet Things J.*, vol. 1, no. 1, pp. 22–32, Feb. 2014.
- [6] A. Sharif, J. Ouyang, F. Yang, H. T. Chattha, M. A. Imran, A. Alomainy, and Q. H. Abbasi, "Low-cost inkjet-printed UHF RFID tag-based system for Internet of Things applications using characteristic modes," *IEEE Internet Things J.*, vol. 6, no. 2, pp. 3962–3975, Apr. 2019.
- [7] D. Muirhead, M. A. Imran, and K. Arshad, "Insights and approaches for low-complexity 5G small-cell base-station design for indoor dense networks," *IEEE Access*, vol. 3, pp. 1562–1572, Aug. 2015.

- [8] W. Saad, M. Bennis, and M. Chen, "A vision of 6G wireless systems: Applications, trends, technologies, and open research problems," *IEEE Netw.*, to be published.
- [9] M. R. Palattella, M. Dohler, A. Grieco, G. Rizzo, J. Torsner, T. Engel, and L. Ladid, "Internet of Things in the 5G era: Enablers, architecture, and business models," *IEEE J. Sel. Areas Commun.*, vol. 34, no. 3, pp. 510–527, Mar. 2016.
- [10] G. M. S. Amendola, M. C. Caccami, A. Caponi, L. Catarinucci, V. Cardellini, E. Di Giampaolo, S. Manzari, F. Martinelli, S. Milici, and C. Occhiuzzi, "RFID & IoT: A synergic pair," *IEEE RFID Virtual J.*, no. 8, pp. 1–21, Mar. 2015.
- [11] S. Vitturi, C. Zunino, and T. Sauter, "Industrial communication systems and their future challenges: Next-generation Ethernet, IIoT, and 5G," *Proc. IEEE*, vol. 107, no. 6, pp. 944–961, May 2019.
- [12] A. Alarifi, A. Al-Salman, M. Alsaleh, A. Alnafessah, S. Al-Hadhrami, M. A. Al-Ammar, and H. S. Al-Khalifa, "Ultra wideband indoor positioning technologies: Analysis and recent advances," *Sensors*, vol. 16, no. 5, p. 707, May 2016.
- [13] T. Pham, M. Tsai, D. Nguyen, C. Dow, and D. Deng, "A cloud-based smart-parking system based on Internet-of-Things technologies," *IEEE Access*, vol. 3, pp. 1581–1591, 2015.
- [14] L.-M. Ang, K. P. Seng, G. K. Ijamaru, and A. M. Zungeru, "Deployment of IoV for smart cities: Applications, architecture, and challenges," *IEEE Access*, vol. 7, pp. 6473–6492, 2018.
- [15] A. Gyrard, A. Zimmermann, and A. Sheth, "Building IoT-based applications for smart cities: How can ontology catalogs help?" *IEEE Internet Things J.*, vol. 5, no. 5, pp. 3978–3990, Oct. 2018.
- [16] T. S. Brisimi, C. G. Cassandras, C. Osgood, I. C. Paschalidis, and Y. Zhang, "Sensing and classifying roadway obstacles in smart cities: The street bump system," *IEEE Access*, vol. 4, pp. 1301–1312, 2016.
- [17] B. Jioudi, E. Sabir, F. Moutaouakkil, and H. Medromi, "Congestion awareness meets zone-based pricing policies for efficient urban parking," *IEEE Access*, vol. 7, pp. 161510–161523, 2019.
- [18] P. Masek, J. Masek, P. Frantik, R. Fujdiak, A. Ometov, J. Hosek, S. Andreev, P. Mlynek, and J. Misurec, "A harmonized perspective on transportation management in smart cities: The novel IoT-driven environment for road traffic modeling," *Sensors*, vol. 16, no. 11, p. 1872, Nov. 2016.
- [19] A. Bagula, L. Castelli, and M. Zennaro, "On the design of smart parking networks in the smart cities: An optimal sensor placement model," *Sensors*, vol. 15, no. 7, pp. 15443–15467, 2015.
- [20] L. Batistic and M. Tomic, "Overview of indoor positioning system technologies," in *Proc. 41st Int. Conf. Inf. Commun. Technol., Electron. Microelectron. (MIPRO)*, 2018, pp. 473–478.
- [21] R. F. Brena, J. P. García-Vázquez, C. E. Galván-Tejada, D. Muñoz-Rodríguez, C. Vargas-Rosales, and J. Fangmeyer, Jr., "Evolution of indoor positioning technologies: A survey," *J. Sensors*, vol. 2017, Mar. 2017, Art. no. 2630413.
- [22] Z. Song, G. Jiang, and C. Huang, "A survey on indoor positioning technologies," in *Theoretical and Mathematical Foundations of Computer Science*, vol. 164. Berlin, Germany: Springer, 2011, pp. 198–206.
- [23] M. Yavari and B. G. Nickerson, "Ultra wideband wireless positioning systems," *Fac. Comput. Sci., Univ. New Brunswick, Fredericton, NB, Canada, Tech. Rep. TR14-230*, 2014.
- [24] "Choosing the optimum architecture for UWB RTLS," Zebra Technol., Lincolnshire, IL, USA, 2013. Accessed: Oct. 10, 2019. [Online]. Available: <https://www.zebra.com/content/dam/zebra/white-papers/en-us/uwb-architecture-en-us.pdf>
- [25] *Application Note: Real Time Location Systems APS003 an Introduction This document is Subject to Change Without Notice Introduction to Real Time Location Systems*, 2014.
- [26] *Positioning and Location-Awareness in 5G*. Accessed: Nov. 24, 2019. [Online]. Available: <http://www.tut.fi/5G/positioning/>
- [27] G. G. Diaz, V. M. Peruzzi, F. R. Masson, and P. S. Mandolesi, "Compact ultra-wideband printed inverted-F antenna for location systems," in *Proc. Argentine Conf. Autom. Control*, 2018, pp. 1–6.
- [28] W. Liu, E. Lupito, Y. L. Sum, B. Tay, and W. Y. Leong, "Ultra wideband antenna for real time location system application," in *Proc. IECON Ind. Electron. Conf.*, 2009, pp. 2738–2742.
- [29] Y. Huang and K. Boyle, *Antennas: From Theory to Practice*. Hoboken, NJ, USA: Wiley, 2008.
- [30] C. A. Balanis, *Antenna Theory: Analysis and Design*, 3rd ed. Hoboken, NJ, USA: Wiley, 2009.
- [31] C. A. Balanis, *Antenna Theory: Analysis and Design*, 4th ed. Hoboken, NJ, USA: Wiley, 2016.
- [32] F. T. Ulaby, R. K. Moore, and A. K. Fung, *Microwave Remote Sensing Active and Passive: Microwave Remote Sensing Fundamentals and Radiometry*, vol. 1. Reading, MA, USA: Addison-Wesley, 1981.
- [33] *DWM1000 Datasheet—Decawave*. Accessed: Nov. 24, 2019. [Online]. Available: <https://www.decawave.com/dwm1000/datasheet/>
- [34] *DWM1001 Datasheet—Decawave*. Accessed: Nov. 24, 2019. [Online]. Available: <https://www.decawave.com/dwm1001/datasheet/>
- [35] E. B. Nogueira, M. H. C. Dias, M. Huchard, F. Nadagijimana, and T. P. Vuong, "Improving the localization accuracy of RSSI-based RTLS by using diversity antenna techniques," in *IEEE MTT-S Int. Microw. Symp. Dig.*, 2013, pp. 1–5.
- [36] E. B. Nogueira, M. Huchard, F. Nadagijimana, and T. P. Vuong, "Optimizing the localization accuracy of a RTLS sensor node by using a metal reflector," in *Proc. 6th Eur. Conf. Antennas Propag. (EuCAP)*, 2012, pp. 3026–3029.



**ABUBAKAR SHARIF** received the M.Sc. degree in electrical engineering from the University of Engineering and Technology, Lahore, Pakistan, and the Ph.D. degree in electronics engineering from the University of Electronic Science and Technology of China (UESTC). From 2011 to 2016, he worked as a Lecturer with Government College University Faisalabad (GCUF), Pakistan. He is also working as a Research Fellow with UESTC. He is the author of several peer-reviewed international journal and conference papers. His research interests include wearable and flexible sensors, compact antenna design, antenna interaction with the human body, antenna and system design for RFID, phased array antennas, passive wireless sensing, and the Internet of Things (IoT).



**JINHAO GUO** received the B.Sc. and M.Sc. degrees in electronics engineering with a focus on electromagnetic field and microwave technology electrical engineering from the University of Electronic Science and Technology of China (UESTC). He is currently working as a Research Fellow with UESTC. He is also working as the Manager of Xiaomi Telecommunications. His research interests include compact antenna design, antenna interaction with the human body, antenna system design for RFID, passive wireless sensing, and the Internet of Things (IoT).



**JUN OUYANG** received the Ph.D. degree in electromagnetic and microwave technology from the University of Electronic Science and Technology of China (UESTC), in 2008, and the Postdoctorate degree in information and signal processing from UESTC, in 2011. He is currently working as an Associate Professor with the School of Electronic Science and Engineering, UESTC. He is also the Associate Director of the Smart Cities Research Center, UESTC. He is also a Research Fellow and the Chief Scientist of the Internet of Things Technology with the Chengdu Research Institute. He is the author of more than 80 articles and 20 patents. Recently, he is leading several national-level research projects, provisional and ministerial research projects. His research interests include antenna theory and design, microwave system, RFID tag, wireless sensing, and the Internet of Things.



**SHENG SUN** (S'02–M'07–SM'12) received the B.Eng. degree in information engineering from Xi'an Jiaotong University, Xi'an, China, in 2001, and the Ph.D. degree in electrical and electronic engineering from Nanyang Technological University (NTU), Singapore, in 2006.

From 2005 to 2006, he was with the Institute of Microelectronics, Singapore. From 2006 to 2008, he was a Postdoctoral Research Fellow with NTU. He was a Humboldt Research Fellow with the

Institute of Microwave Techniques, University of Ulm, Ulm, Germany, from 2008 to 2010, and a Research Assistant Professor with The University of Hong Kong, Hong Kong, from 2010 to 2015. Since 2015, he has been the Young Thousand Talents Plan Professor with the University of Electronic Science and Technology of China, Chengdu, China. He has coauthored one book and two book chapters, and over 140 journal and conference publications. His current research interests include electromagnetic theory, computational mathematics, multiphysics, numerical modeling of planar circuits and antennas, microwave passive and active devices, and the microwave- and millimeter-wave communication systems. He is currently a member of the Editor Board of the *International Journal of RF and Microwave Computer Aided Engineering* and the *Journal of Communications and Information Networks*. He was a recipient of the ISAP Young Scientist Travel Grant, Japan, in 2004, the General Assembly Young Scientists Award from the International Union of Radio Science, in 2014, and the Hildegard Maier Research Fellowship of the Alexander Von Humboldt Foundation, Germany, in 2008. He was a co-recipient of the several best paper awards at international conferences. He received the Outstanding Reviewer Award from the IEEE MICROWAVE AND WIRELESS COMPONENTS LETTERS, in 2010. He was the Associate Editor of the IEICE TRANSACTIONS ON ELECTRONICS, from 2010 to 2014, and the Guest Associate Editor of the *Applied Computational Electromagnetics Society's Journal*, in 2017. He is also an Associate Editor of the IEEE MICROWAVE AND WIRELESS COMPONENTS LETTERS.



**KAMRAN ARSHAD** (SM'15) is currently the Dean of Graduate Studies and Research and a Professor in electrical engineering with Ajman University, United Arab Emirates. Prior to join Ajman University, in January 2016, he has been Associated with the University of Greenwich, U.K., as a Senior Lecturer and the Program Director of M.Sc. Wireless Mobile Communications Systems Engineering. He is also a Senior Fellow of the U.K. Higher Education Academy (SF-HEA). He is an

Associate Editor of the *EURASIP Journal on Wireless Communications and Networking*. He led a number of locally and internationally funded research projects encompassing the areas of cognitive radio, LTE/LTE-Advanced, 5G, Optimization and cognitive Machine-to-Machine (M2M) communications. He has contributed to several European and international large-scale research projects. He has over 130 technical peer-reviewed articles in top quality journals and international conferences, received three Best Paper Awards, one best Research and Development Track Award, and chaired technical sessions in several leading international conferences.



**MUHAMMAD ALI IMRAN** (M'03–SM'12) received the M.Sc. (Hons.) and the Ph.D. degrees from the Imperial College London, U.K., in 2002 and 2007, respectively. He is currently the Vice Dean Glasgow College, UESTC, and a Professor of communication systems with the School of Engineering, University of Glasgow. He is also an Affiliate Professor with The University of Oklahoma, USA, and a Visiting Professor with the 5G Innovation Centre, University of Surrey,

U.K. He has over 18 years of combined academic and industry experience, working primarily in the research areas of cellular communication systems. He received the Award of Excellence in recognition for his academic achievements, conferred by the President of Pakistan. He also received the IEEE Comsoc's Fred Ellersick Award, in 2014, the FEPS Learning and Teaching Award, in 2014, and the Sentinel of Science Award, in 2016. He has been awarded 15 patents, has authored/coauthored over 300 journal and conference publications, and has been a Principal/Co-Principal Investigator on over £six million in sponsored research grants and contracts. He is also the Editor/Co-Editor of two books *Access, Fronthaul and Backhaul Networks for 5G and Beyond* (IET, ISBN 9781785612138) and *Energy Management in Wireless Cellular and Ad-hoc Networks* (Springer, ISBN 9783319275666).



**QAMMER H. ABBASI** (S'08–M'12–SM'16) received the Ph.D. degree in electronic and electrical engineering from the Queen Mary University of London (QMUL), U.K., in January 2012. From 2012 to June 2012, he was a Postdoctoral Research Assistant with the Antenna and Electromagnetics Group, QMUL, U.K. From 2012 to 2013, he was an International Young Scientist under the National Science Foundation China (NSFC), and an Assistant Professor with the University of

Engineering and Technology (UET), KSK, Lahore. From August 2013 to April 2017, he was with the Center for Remote Healthcare Technology and the Wireless Research Group, Department of Electrical and Computer Engineering, Texas A&M University (TAMUQ), initially as an Assistant Research Scientist and later was promoted to an Associate Research Scientist and a Visiting Lecturer. His research interests include nano communication, the Internet of Things, 5G and its applications to connected health, RF design and radio propagation, RFID, applications of millimeter and terahertz communication in healthcare and agri-tech, wearable and flexible sensors, compact antenna design, antenna interaction with human body, implants, body-centric wireless communication issues, wireless body sensor networks, non-invasive health care solutions, and physical-layer security for wearable/implant communication. He received several recognitions for his research. He was the Chair of IEEE Young Professional Affinity Group. He is also the Associate Editor for IEEE ACCESS, the IEEE JOURNAL OF ELECTROMAGNETICS, RF AND MICROWAVES IN MEDICINE AND BIOLOGY, *Advanced Electromagnetics Journal* and acted as the Guest Editor for numerous special issues in top-notch journals, including *Elsevier Nano Communication Network*. He is a currently a Lecturer (an Assistant Professor) with the School of Engineering, University of Glasgow and a Visiting Lecturer (an Assistant Professor) with the Queen Mary, University of London (QMUL). He has grant portfolio of around £3.5M, contributed to a patent and more than 200 leading international technical journal and peer-reviewed conference article, in addition to five books. He is also a member of IET, in 2012.

...